Mechanism of Vibrational Energy Dissipation of Free OH Groups at the Air-Water Interface

Cho-Shuen Hsieh[1, 2, *], R. Kramer Campen[3], Masanari Okuno[2], Ellen H. G. Backus[2], Yuki Nagata[2], and Mischa Bonn[2, †]

[1]FOM Institute AMOLF, Science Park 104, 1098 XG Amsterdam, The Netherlands [2]Max-Planck Institute for Polymer Research, Ackermannweg 10, 55128 Mainz, Germany [3]Fritz Haber Institute of the Max Planck Society, Faradayweg 4-6, 14195 Berlin, Germany [*]hsieh@amolf.nl, [†]bonn@mpip-mainz.mpg.de

Submitted to Proceedings of the National Academy of Sciences of the United States of America

Interfaces of liquid water play a critical role in a wide variety of processes that occur in biology, technology and the environment. Many macroscopic observations clarify that the properties of liquid water interfaces significantly differ from those of the bulk liquid. While the intermolecular interactions of interfacial molecules generally differ from those in bulk, understanding the interfacial molecular structure of liquid water is crucial. Vibrational sum frequency (VSF) spectroscopy in principle allows access to this information, but understanding the impact of structure (and structural dynamics) on the observed line shapes is extremely challenging. A prerequisite to such understanding is a quantitative description of the timescales and mechanisms of the vibrational relaxation of interfacial water. Here we elucidate the rate and mechanism of vibrational energy dissipation of water molecules at the air-water interface using femtosecond two-color vibrational sum-frequency (VSF) spectroscopy. Vibrational relaxation of non-hydrogen bonded OH groups occurs at a sub-picosecond time scale in a manner fundamentally different from hydrogen-bonded OH groups in bulk, through two competing mechanisms: intramolecular energy transfer (IET) and ultrafast reorientational motion that leads to free OH groups becoming hydrogen-bonded. Both pathways effectively lead to the transfer of the excited vibrational modes from free to hydrogen-bonded OH groups, from which relaxation readily occurs. Of the overall relaxation rate of interfacial free OH groups at the air-H2O interface 2/3 is explained by IET, while the remaining 1/3 is dominated by the reorientational motion.

sum frequency generation | vibrational spectroscopy | energy relaxation | reorientation

Introduction:

Interfaces of liquid water play an important role in a wide variety of biological, environmental and technological processes (1–3). More than sixty years of study have shown that these interfaces have many unusual macroscopic properties – e.g. the high surface tension, the tendency to sequester ions of the air/water interface, and the high proton conductivity of the membrane water interface – that are difficult to understand given simple descriptions of bulk liquid water. Driven by the desire to explain such observations, several decades have been spent trying to understand the molecular level structure and dynamics of water at aqueous interfaces.

Experimentally probing interfacial water molecular structure and dynamics is a formidable challenge. Performing similar measurements at solid surfaces in ultra-high vacuum (UHV) is easier: electrons, photons, or atoms can be brought to, and retrieved from, the surface through vacuum(4). Recently notable progress has been made in employing UHV surface science tools to the vacuum/liquid water interface by interrogating liquid jets in vacuum(5–8). While this approach has provided important insight, the experimental geometry is not applicable to aqueous interfaces more generally: e.g. one cannot probe water/organic liquid interfaces using this approach.

Because vibrational spectroscopy has no intrinsic requirement for vacuum and because the frequency and intensity of the OH stretch change dramatically as a function of local environment, probing the spectral response of the OH stretch of H_2O has proven extremely useful in characterizing the structure and dynamics of bulk liquid water (9–13). Problematically conventional vibrational spectroscopies (i.e. infrared (IR) absorption or spontaneous Raman) cannot generally be used to probe an aqueous interface: because they lack interfacial specificity it is generally difficult to distinguish the response of H_2O molecules at the interface from the much larger number in bulk. This challenge was initially overcome by Shen and coworkers in 1991 by employing the laser based technique, vibrational sum frequency (VSF) spectroscopy to probe the air/water interface(14).

In a VSF experiment, an IR pulse is overlapped at the surface in both time and space with a visible (VIS) pulse and the output at the sum of the frequencies of the two incident fields monitored. This VSF emission is, within the dipole approximation, interface specific in media with bulk inversion symmetry and is a spectroscopy because it increases in intensity by $> 10^4$ when the frequency of the incident IR is tuned in resonance with a normal mode of the molecules at an interface(15). As initially shown by Shen and coworkers, and subsequently a variety of others, because the quadrupole response from liquid water is relatively low, VSF spectroscopy can furnish the OH stretch response of just the water molecules within 1-2 layers of an interface (16–18).

Because of its environmental ubiquity, experimental simplicity and its relevance to understand hydrophobic solvation more generally, much work has focused on the spectral response of interfacial water at the air/water interface(19–21). A VSF spectrum (Fig. 1) for the air/water interface shows a broad band at lower frequency (3100-3500 cm^{-1}), attributed to H-bonded OH groups,

Significance

Interfaces of liquid water play an important role in a wide variety of biological, environmental and technological processes. The aqueous interfaces have many unusual macroscopic properties e.g. the high surface tension, the tendency to sequester ions of the air/water interface, and the high proton conductivity that are difficult to understand given simple descriptions of bulk liquid water. To unveil the driving force to differentiate the interfacial water from the bulk water, the molecular level structure and dynamics of water at the interfaces are crucial. Here we study the dynamics of the vibrational energy relaxation by using the ultrafast time-resolved surface specific vibrational spectroscopic technique and show that rather unique vibrational relaxation pathways contribute to the energy dissipation of interfacial water.

Reserved for Publication Footnotes

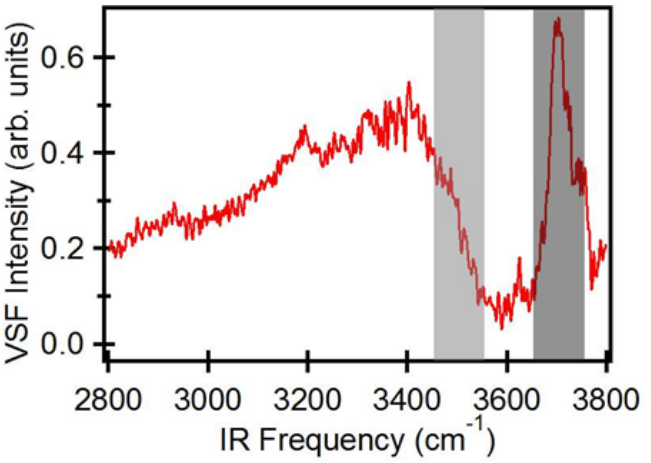

Fig. 1. Static VSF spectrum of the air-H_2O interface. Dark grey and light grey rectangles mark the spectral region of free and H-bonded OH, respectively, that are excited and detected in the pump-probe experiments.

and a narrow peak at higher frequency (~3700 cm^{-1}), attributed to free OH groups(20, 22–24). While it is clear that these spectral features report on the structure of interfacial water, extracting this structural information from the measured response has proven extremely challenging. This challenge is not unique to the VSF spectral response of interfacial water. It can be straightforwardly demonstrated that, for a particular resonance apparent in any one–dimensional (frequency) vibrational spectrum, the extent to which inhomogeneous broadening, anharmonic coupling to other modes, and chromophore motion influence the observed spectral response cannot be unambiguously determined(25). As a consequence the extent to which a spectrum is influenced by molecular structure cannot be unambiguously defined. Much prior work has shown that all of these factors influence the VSF spectral response of interfacial water. In particular, significant inter- and intramolecular coupling is known to dominate the hydrogen bonded portion of the spectrum and water molecule motion is known to occur on sub ps time scales(26–28). The fact that multiple possible effects may explain the observed spectral response of interfacial water has been clearly demonstrated, for the low frequency portion (≈ 3100 cm^{-1}) of the hydrogen bonded OH at the air/H_2O interface, by the Morita and Skinner groups who have shown that the experimental spectral response can be equally well reproduced by computational models with quite different underlying physics(17, 29).

Restricting ourselves to the free OH – which prior work has found to be well described as a single homogenously broadened resonance that interacts only weakly with its environment(30) – clearly understanding changes in peak amplitude or width with changes in aqueous solution composition requires understanding the physical controls on line width: the degree to which the measured free OH spectral response is controlled by pure dephasing and vibrational lifetime. Because the vibrational relaxation mechanism is interfacial structure dependent, if lifetime is sufficiently long to influence the free OH spectral response knowledge of the relaxation mechanism is also important.

Because it is particularly important in understanding hydrophobic solvation and because, as discussed above, prior work strongly suggests it should be simpler, we focus initially on understanding the influence of interfacial water structure and structural dynamics on the free OH peak shown in Figure 1. Changes in the free OH resonance peak amplitude or width are routinely observed with changes in aqueous solution composition(23, 24). To correctly interpret and understand these changes evidently requires understanding the physical factors determining the line width, that is, the degree to which the measured free OH spectral response is controlled by pure dephasing (elastic interactions typically with low-frequency mode that modulate the free OH frequency) and the free OH vibrational energy lifetime.

To deconvolute the relative influence of vibrational lifetime and pure dephasing on the lineshape, a method of directly measuring one of these two quantities with interfacial specificity is required. We and others have recently applied a time-resolved ultrafast IR-pump/VSF-probe scheme to elucidate vibrational energy relaxation dynamics of OH groups at a variety of interfaces (31–35). In these experiments, an IR pump pulse excites OH groups at a specific vibrational frequency, and the effect of that excitation is followed in time with the VSF probe pulse pair. For the excited OH groups, the VSF intensity is temporarily decreased ('bleach'), and the recovery of the signal is a result of vibrational relaxation. For the free OH both at the air/water and hydrophobic self-assembled monolayer/water interface, slow relaxation (0.85 – 1.2 ps) has been reported(31, 35). As the homogenous dephasing time (T_2) of the free OH is 221 fs (given a measured FWHM in Fig. 1 and assuming inhomogeneous contributions to the line width are negligibly small) it is clear that the line width of the free OH spectral response is influenced by vibrational lifetime and thus that revealing changes in free OH spectral response with aqueous phase composition or with the composition of the adjoining phase requires understanding the free OH vibrational relaxation mechanism.

Three possible relaxation pathways can be identified. Previously we have shown that free OH groups reorient on a timescale (≈ 1 ps) very similar to vibrational relaxation(35, 36). This observation suggests that one possible relaxation mechanism is the rotation of excited OH groups towards the bulk and formation of a hydrogen bond after which energy dissipation occurs rapidly as a result of the increased anharmonicity of the O-H vibrational potential. In what follows we term this mechanism the REOR vibrational relaxation pathway. A second relaxation mechanism has been proposed from the appearance of the cross peaks in two-dimensional VSF spectra of D_2O at the air-D_2O interface: the vibrational energy of the free OD is transferred to the H-bonded OD in the same D_2O molecule, which is weakly H-bonded, on sub-picosecond timescales(34). Hereafter we describe this as the intramolecular energy transfer (IET) relaxation pathway. Finally, in liquid water much prior experimental and computational work has shown that the vibrational relaxation of the OH stretch proceeds through the overtone of the bending mode, to the bend fundamental, to whole molecule librations(27). Absent additional information it seems plausible that relaxation of the excited free OH might occur in a similar manner; in what follows we term this mechanism the intramolecular vibrational relaxation (IVR) pathway. These mechanisms are schematically illustrated in Fig. 2.

In this study we resolve the relative roles of these mechanisms in the vibrational relaxation of interfacial free OH groups at the air/water interface. By analyzing two-color time-resolved VSF signals we show that the exchange of excited vibrational energy between free OH and H-bonded OH occurs on a sub-picosecond timescale. Using isotopically diluted water, we suppress intra- and intermolecular coupling while leaving structural relaxation processes relatively unaffected. Our results show that IET explains 2/3 of the vibrational relaxation of the free OH groups in pure H_2O while the remaining 1/3 is the result of REOR.

As noted above, VSF spectra of interfacial water does not uniquely determine interfacial structure. Our quantification of vibrational lifetime and relaxation mechanism provides an important additional piece of information to evaluate otherwise equally plausible descriptions of the physical mechanisms underlying the spectral response. More generally, as alluded to above, much prior work seems to suggest that the free OH

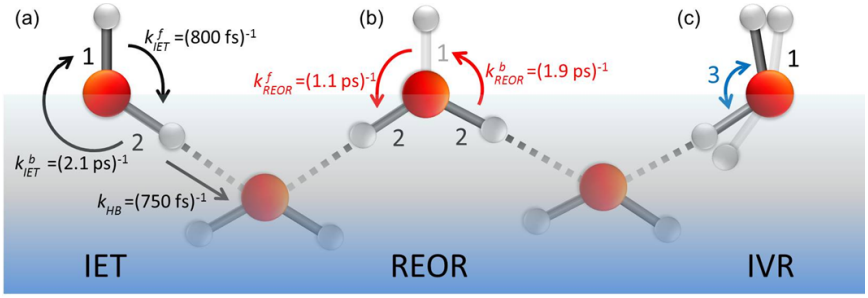

Fig. 2. Schematically depicting the pathways for vibrational relaxation of free OH groups. (a) Intramolecular energy transfer (IET), which indicates the energy coupling between free OH (label 1) and H-bonded OH (label 2). (b) Reorientational motion of the free OH (label 1) which rotates into the bulk and forms a hydrogen bond (REOR). (c) Intramolecular vibrational relaxation (IVR), which represents the coupling between the free OH stretching (label 1) and the bending modes (label 3) of the water molecules.

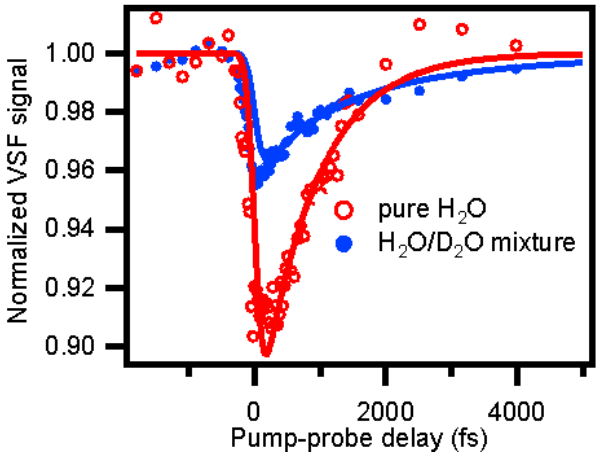

Fig. 3. IR-pump/VSF-probe data for excitation and detection of free OH groups at the air-water interface for pure (red, open circles) and isotopically diluted H_2O (H_2O:D_2O = 1:1, blue, filled circles). The red curve is the monoexponential fitting of the pure H_2O sample and the blue curve is the biexponential fitting of the H_2O-D_2O mixture, which shows that the time constant of the vibrational relaxation of free OH for H_2O and HDO are 840 fs and 2.6 ps, respectively. Both fit curves are convoluted with the system response.

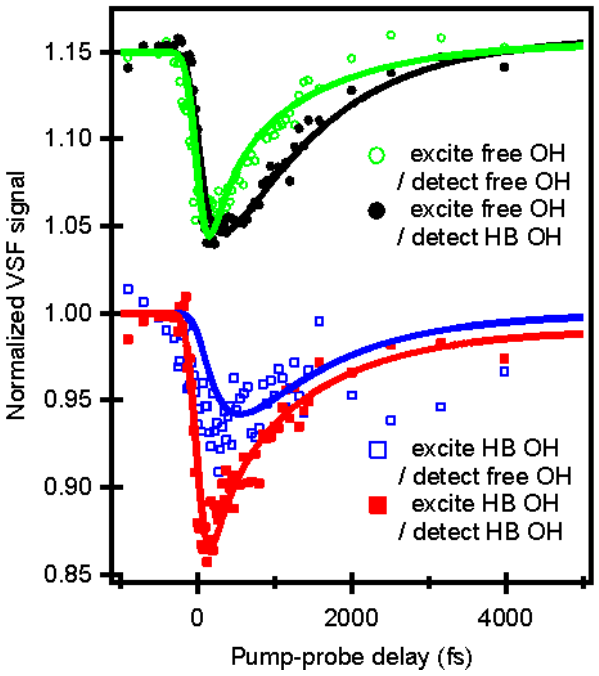

Fig. 4. IR-pump/VSF-probe data for free OH and H-bonded (HB) OH groups at the air-water interface. The upper two traces are data with 3700 cm^{-1} IR pump/3700 cm^{-1} (green, open circles) and 3500 cm^{-1} (black, filled circles) probes, while the lower two traces are data with 3500 cm^{-1} IR pump/3700 cm^{-1} (blue, open squares) and 3500 cm^{-1} (red, filled squares) probes. Solid lines are fits with a vibrational relaxation model (for details, see supplemental material). The green and black curves have an offset of 0.15.

plays an important role in the free energy of solvation of objects ranging from small hydrophobic moieties, to large amphiphilic macromolecules (such as proteins) to extended hydrophobic and amphiphilic surfaces(37). Since this free energy of solvation is thought to be an important driving force in processes as diverse as protein folding, colloidal aggregation and hydrophobic collapse, the quantitative understanding we here gain of what, exactly, controls the interfacial free OH spectral response, what we probe when we probe the free OH, seems likely to be of interest to a wide community of bio- and soft matter chemists and physicists.

Results and discussion:

To study the vibrational energy dynamics of the free OH group (dark grey area in Fig. 1), we excite these OH groups at ~3700 cm^{-1} with an IR pump pulse and probe the response with VSF probe pulse pair as a function of delay time. The data, after integrating the measured VSF intensity from 3650 cm^{-1} to 3750 cm^{-1} (with respect to the IR probe frequency, red curve in Fig. 3), show a 10% bleach which recovers on a sub-ps timescale. A single-exponential fit to the data gives a time constant for the recovery of the VSF signal of T_{H_2O} = 840 ± 50 fs for the free OH in pure H_2O. This timescale can of course be a result of a combination of the three prospective relaxation pathways: IET, REOR, and IVR. Put in more formal notation, we expect that $k_{VR}^{(H_2O)} = k_{IET}^{(H_2O)} + k_{IVR}^{(H_2O)} + k_{REOR}^{(H_2O)} = (0.84\ \text{ps})^{-1}$, where k is the rate constant associated with the energy relaxation process and we have lumped together the IET and IVR pathways into a single term for reasons that will become clear below.

To help us quantify the contribution of each of these pathways we require an experiment that allows us to selectively switch one (or more) off. To do so we next performed a similar IR pump / VSF probe experiment probing the free OH of HOD at the air/water interface. Because of the large energy mismatch between the OH and OD stretch and the HOD, H_2O and D_2O bend frequencies(38), neither near resonant energy transfer between the OD and OH stretch on the same water molecule nor relaxation from the OH stretch through the overtone of the bend is probable in HOD. Put another way, in HDO we expect the IET and IVR pathways to be shut down ($k_{IET}^{(HDO)} = k_{IVR}^{(HDO)} = 0$) and vibrational relaxation to be therefore dominated by REOR.

The blue curve in Fig. 3 displays the IR-pump/VSF-probe result for exciting and probing the free OH stretching mode at the air-water interface for a H_2O-D_2O mixture (1:1 molar ratio). As is clear from inspection, the timescale of VSF signal recovery is much slower for the mixture than pure H_2O (the red curve).

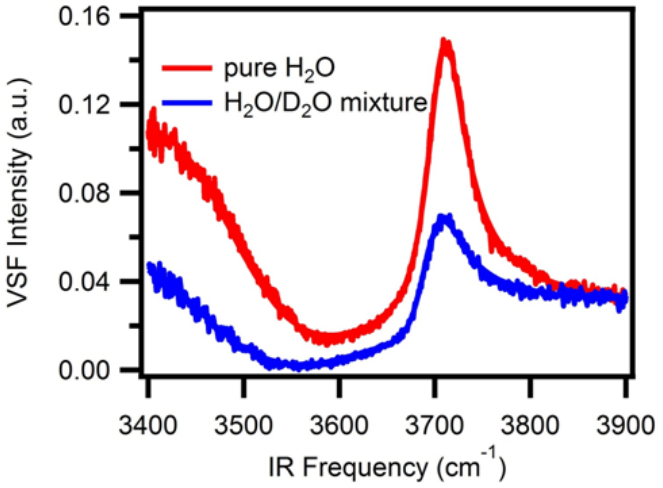

Fig. 5. VSF spectrum of pure (red) and isotopically diluted H_2O (H_2O:D_2O=1:1, blue) and their spectral fitting curves.

This qualitative observation strongly suggests that both the IET and/or IVR pathways are important in describing the vibrational relaxation of the free OH of H_2O. To quantify the importance of IET/IVR relative to REOR we need to fit the data. For the H_2O-D_2O mixture (given a small interfacial isotope fractionation(39)), half of the free OH groups in our excitation volume are part of an H_2O molecule; the other half are part of HDO(40). Assuming these two types of free OH groups contribute equally to the measured signal from the mixture, and therefore fitting this data using a biexponential with two equal amplitudes and taking T_{H_2O}= 840 fs for free OH in H_2O, we find that the timescale of signal recovery of the free OH in HDO, T_{HDO}, is 2.6 ± 0.3 ps: three times slower than that of the free OH in H_2O. Taking, $k_{IET}^{(HDO)}=k_{IVR}^{(HDO)}=$ 0, and assuming that the reorientation rate of an OH group in HDO is similar to that of an OH group in H_2O we thus have $k_{REOR}^{(HDO)}=k_{REOR}^{(H_2O)}=$ (2.6 ps)$^{-1}$. Recalling that, $k_{VR}^{(H_2O)}= 1/T_{H_2O}$ = (0.84 ps)$^{-1}$, we obtain $k_{IET/IVR}^{(H_2O)}=k_{VR}^{(H_2O)}-k_{REOR}^{(H_2O)}=$ (1.24 ps)$^{-1}$.

Because both IET and IVR are suppressed in HOD quantifying the relative importance of these two pathways requires different types of experiments. Here we do so by performing an IR pump / VSF probe experiment in which we excite the free OH (i.e. the frequency range shown in the dark grey rectangle) and probe the blue side (weakly hydrogen bonded) of the hydrogen bonded OH spectral response (i.e. the light grey rectangle in Fig. 1). Prior work has shown that this frequency range corresponds to the OH stretch of the hydrogen bonded half of a water molecule that contains a free OH(41).

The IR (free OH) pump/VSF (weakly hydrogen bonded) trace, with probe intensities integrated from 3450 cm^{-1} to 3550 cm^{-1}, is shown in black in Fig. 4. For comparison the free OH IR pump and free OH VSF probe is shown as a green curve in Fig. 4 (same data as red curve in Fig. 3). Three qualitative features of the comparison are readily apparent: there is a ∼ 300 fs delay between the directly free OH pumped signal (green trace) and the coupling signal (black trace), the bleach magnitudes (the signal size) is similar for both experiments and both traces have an initial bleach followed by a monotonic recovery. This relatively small delay between the pumped and coupling traces is consistent with a scenario in which vibrational energy is effectively transferred from the free OH to weakly H-bonded OH populations by energy transfer and/or reorientation of free OH groups to become H-bonded. Similarly, the nearly identical size of the bleach for both signals suggests that no energy is lost from the system in this transfer: that the great majority of the vibrational excitation deposited in the free OH is transferred to the bond stretch modes of OH groups that are weak hydrogen bond donors. Because vibrational relaxation of the free OH through IVR would require energy to leave the free OH stretch and move rapidly into the bend fundamental (i.e. well outside of our probe window) both of these observations thus suggest that IVR is relatively unimportant in describing free OH relaxation. Finally, we note that prior works have shown that the interfacial hydrogen bonded OH stretch shifts to higher frequencies when heated(22). If vibrational relaxation and subsequent thermalization of the free OH excitation were sufficiently rapid we would expect to see a transient increase, rather than decrease and recovery, in the coupling trace. Clearly the data are inconsistent with such rapid thermalization.

This comparison between the free OH pump / free OH probe and free OH pump / weakly H bonded OH probe traces thus suggests a picture in which a free OH group is initially excited and this excitation is either transferred to the hydrogen bonded OH group on the other half of the same molecule or the excited OH group rotates down and forms a hydrogen bond. Clearly, however, this is only the first part of the vibrational relaxation pathway. To investigate what happens next we performed two additional IR pump / VSF probe experiments: one in which weakly hydrogen bonded OH groups are pumped and the free OH probed (blue trace in Fig. 4) and one in which weakly hydrogen bonded groups are both pumped and probed (red trace in Fig. 4). Interestingly, these two signals (the two bleach amplitudes) are notably different: the bleach for the free OH is appreciably smaller than for the H-bonded OH probe. This difference suggests that, on excitation of weakly hydrogen bonded OH groups some energy transfer likely occurs via IET or REOR to the higher energy free OH group while the rest, possibly through rapid intermolecular energy transfer to more strongly hydrogen bonded OH stretches on other water molecules or IVR, dissipates through other channels.

Taken as a whole the data discussed thus far suggests that free OH vibrational relaxation proceeds by IET and REOR (but not IVR) and that there is an effective time constant of (1.24 ps)$^{-1}$ associated with the IET pathway and (2.6 ps)$^{-1}$ with the REOR. As discussed above, these data further suggest that these time constants are a combination of forward and backward rates for both processes: an initially excited free OH group that has either reoriented to form a hydrogen bond or transferred its excitation to the hydrogen bonded OH group on the same molecule can either rotate back to become free or transfer its excitation back to the free OH on ultrafast time scales. We have previously shown in experiment and simulation that the characteristic time for a free OH to rotate towards bulk liquid and form a hydrogen bond is ≈ 1 ps(35, 36). On the face of it the (2.6 ps)$^{-1}$ time constant associated with the REOR pathway appears to conflict with this previous observation. To explore whether the (2.6 ps)$^{-1}$ could be the result of this observable convoluting both forward and backward rates, we developed a model to account explicitly for the possibility of a return of the excitation to the free OH either because the newly hydrogen bond OH is once again free or because of excitation transfer back from a hydrogen bonded OH to the free OH on the same molecule.

To do so we first assume free OH vibrational relaxation occurs in two stages: a first step that is reversible and leads to an initially excited free OH group either becoming (through REOR) or transferring its excitation to (through IET) a weakly hydrogen bonded OH group and a second step that describes the relaxation of the weakly hydrogen bonded OH group (with rate constant k_{HB}) and is non-reversible (for details, see supplemental information and Ref.(34)). Given such assumptions, we wish to ask whether the model can describe all data in Figure 4 simultaneously. The solid lines in Fig. 4 are the results of the model with transfer rate k_{VR}^{f} = (460 ± 50 fs)$^{-1}$, k_{VR}^{b}= (980 ± 100 fs)$^{-1}$, and k_{HB} = (750 fs ± 80

fs)$^{-1}$. The superscript "*f*" denotes the forward process (the excited vibrational stretching mode changes from the free OH to the H-bonded OH) and "*b*" denotes the backward process (the excited vibrational stretching mode changes from the H-bonded OH to the free OH).

As shown above, the excitation transfer from free to H-bonded OH groups, the rate constant of which k_{VR}^{f} = (460 fs)$^{-1}$, is the sum of relaxation via IET (k_{IET}^{f}) and REOR (k_{REOR}^{f}): $k_{VR}^{f} = k_{IET}^{f} + k_{REOR}^{f}$. To solve for the backward rates of both processes we assume that there is no energy barrier and the system is at equilibrium with respect to intramolecular energy transfer, i.e. the ratio of forward to backward rates of IET is related to the frequency difference between these modes, as described in an Arrhenius equation, and is 2.6: $k_{IET}^{f}/k_{IET}^{b} = exp[\hbar(3700\text{-}3500)/k_BT] = 2.6$ at T=300 K. Similarly, if we assume that the relative number of interfacial hydrogen bonded OH groups does not change as a result of the IR pump, and given that the population of H-bonded OHs is 1.7 times larger than the population of free OHs (discussed in detail in the supplemental material), the reorientation rate for the H-bonded OH to break the hydrogen bond and become a free OH must be 1.7 times slower than the converse: $k_{REOR}^{b} = k_{REOR}^{f}/1.7$. Substituting we find, for the free OH to H-bonded OH transition, $k_{VR}^{f} = k_{IET}^{f} + k_{REOR}^{f}$ = (460 fs)$^{-1}$, and for the H-bonded OH to free OH $k_{VR}^{b} = k_{IET}^{b} + k_{REOR}^{b} = k_{IET}^{f}/2.6 + k_{REOR}^{f}/1.7$ = (980 fs)$^{-1}$. Rearranging terms leads to k_{IET}^{f} = (800 fs)$^{-1}$ and k_{REOR}^{f} = (1.1 ps)$^{-1}$. These time constants are summarized in Fig. 2. The 1.1-ps time constant for the reorientational motion of the free OH group and formation of a hydrogen bond thus appears to be consistent with our earlier estimates for the rates of this process(35, 36).

To summarize, we have thus calculated the characteristic rate constant for free OH vibrational relaxation in two ways: a simple exponential fit and a rate model that solves the system of coupled differential equations describing population transfer in a three state model. Summing the forward and backward time constants for each process extracted from the rate model allows direct comparison to the exponential analysis offered above. We find that the time constant of vibrational relaxation of the free OH due to IET calculated using the rate model is $k_{IET}^{f}\text{-}k_{IET}^{b} = k_{IET}^{f}\text{-}k_{IET}^{f}/2.6$ = (1.3 ps)$^{-1}$ and that due to REOR $k_{REOR}^{f}\text{-}k_{REOR}^{b} = k_{REOR}^{f}\text{-}k_{REOR}^{f}/1.7$ = (2.67 ps)$^{-1}$. Clearly both time constants are in good agreement with the exponential description, in which $k_{REOR}^{(H_2O)}$ = (2.6 ps)$^{-1}$ and $k_{IET}^{(H_2O)}$ = (1.24 ps)$^{-1}$, offered above. Both ways of analyzing the data thus appear to reach a similar conclusion: about 1/3 of the vibrational relaxation of the free OHs in H_2O is due to structural relaxation with and the remaining 2/3 to intramolecular energy transfer.

As noted above, prior work suggests that, while inhomogeneous broadening is important in determined the hydrogen bonded OH spectral response at the air/water interface, it is relatively unimportant in understanding the free OH. This then implies that we are justified in describing the VSF spectral response of the free OH at both the air/H_2O and air/H_2O:HOD:D_2O interface as a sum of Lorentzians: $I_{VSF} \propto |\chi_{NR}^{(2)} + \sum_n [A_n/(\omega_{IR} - \omega_n + i\Gamma_n)]|^2$, where A_n, ω_n, and $2\Gamma_n$ are the amplitude, frequency, and full-width-at-half-maximum (FWHM), respectively, of mode n. Γ is related to the decay rate ($1/T_2$) of the polarization (induced by the IR pulse), $2\pi\Gamma = 1/T_2$, where T_2 is the homogeneous dephasing time. This homogenous dephasing time can be decomposed into two contributions, $1/T_2 = 1/(2T_1) + 1/T_2^*$, where T_1 is the population lifetime and T_2^* is the pure dephasing time. The spectral fits in Fig. 5 indicate that the FWHM of the free OH is 48 cm^{-1} (Γ = 24 cm^{-1}) for H_2O and 40 cm^{-1} (Γ = 20 cm^{-1}) for HDO, i.e. a difference of 4 cm^{-1} in Γ. For H_2O the lifetime $T_1 = T_{H_2O}$ = 840 fs results in a contribution of 3.2 cm^{-1} to Γ, while for HDO $T_1 = T_{HDO}$ = 2.6 ps resulting in a contribution of only 1.0 cm^{-1}. As changes in T_1 thus explain only 2.2 cm^{-1} of the 4 cm^{-1} difference in Γ between the spectral response of the interfacial free OH of H_2O and that of HOD, the remaining 1.8 cm^{-1} must be due to differences in the pure dephasing time, T_2^*, of the two systems, presumably due to subtle differences in low frequency modes of the H-bonded network for the isotopologues. As expected the pure dephasing time, T_2^*, of free OH groups both for H_2O, ≈ 250 fs, and HDO, ≈ 280 fs, are 3 times longer than the H-bonded OH of HDO in bulk D_2O (≈ 90 fs)(42), presumably due to the absence of the frequency modulation of free OH groups by the surrounding water molecules at the air-water interface.

Free OH groups at hydrophobic interfaces are important: they are one of few molecular scale observables whose presence correlates with macroscopic indicators of hydrophobicity such as contact angle. To understand how this molecular scale observable connects with macroscopic indicators requires quantitative insight into the structure and dynamics of this species. Vibrational sum frequency spectroscopy is the most straightforward way to observe this free OH experimentally but understanding the physical chemistry underlying this spectral response is challenging. Armed with only a VSF measurement it is not possible to understand what factors control the free OH line shape and therefore understand the implications of changes in lineshape for molecular structure. In this study we show that free OH groups at the air/water interface have a vibrational lifetime of ≈ 850 fs. Two color IR pump / VSF probe measurements of both the free OH of H_2O at the air/H_2O interface and of HOD at the air/H_2O:D_2O mixture interface allow us to clarify that one third of this energy relaxation happens via structural relaxation, the free OH rotates towards the bulk liquid at which point it forms a hydrogen bond, while two thirds is the result of intramolecular energy transfer – excitation transfer from the excited free OH to the hydrogen bonded OH on the other half of the same molecule. Given this knowledge of lifetimes for both species, we further calculate pure dephasing times of 250 fs for free OHs in H_2O and 280 fs for HDO. Taken together this work allows us full insight into the VSF free OH spectral response at the air/water interface: we can now completely specify the factors that control the spectral line shape. Such insight, and similar experiments to those described here for other aqueous solutions, should be invaluable in quantitative description of the VSF OH stretch spectral response and, therefore, in understanding hydrophobic solvation.

Materials and methods:

The IR-pump/VSF-probe setup is in brief described as follows. A Ti:sapphire regenerative amplifier (Spitfire Ace, Spectra-Physics) was used to generate laser pulses centered at 800 nm with a full-width-at-half-maximum (FWHM) of 30 nm and a pulse duration of 40 fs. The amplifier produces ∼5 mJ of energy/pulse with a repetition rate of 1 kHz. Two commercial optical parametric amplifiers (TOPAS-C, Spectra-Physics) are each pumped with 1 mJ of the amplified 800 nm beam. For one TOPAS-C the signal and idler were used in a difference frequency mixing process in a silver gallium disulfide ($AgGaS_2$) crystal, resulting in 3 μJ IR pulses, tunable around a central wavelength of ∼2850 nm (∼3500 cm^{-1}) with a FWHM of 300 cm^{-1}, which was used as IR probe. Another TOPAS-C was used to produce an idler field (2272 nm and 2222 nm). The field was then doubled in a β-barium borate (BBO) crystal and subsequently the difference frequency was generated in a 6 mm thick $KTiOPO_4$ (KTP) crystal with 2 mJ of the 800nm Ti:sapphire output. This produces ∼100 μJ mid-IR pulses (centered at 3500 and 3700 cm^{-1}) with a FWHM of 100 cm^{-1}, used as the pump pulse. The remaining 800 nm pulse of the laser output was narrowed by an etalon (SLS Optics Ltd) to 9 cm^{-1} and was used for the VIS probe. The IR-pump/VSF-probe measurements were made in reflection geometry. The VIS probe, IR probe, and IR pump beams lay in the same plane orthogonal to the air-water interface and had incident angles of 50, 45, and 55 degrees with respect to the surface normal, respectively. The energy of the IR pump, IR probe, and VIS probe at the sample was 40, 1, and 4 μJ/ pulse, respectively. The samples were distilled Millipore filtered H_2O (18MΩ-cm resistivity) mixed with D_2O (Cambridge Isotope Laboratories, Inc., 99.93 % purity, used without further purification) and placed in a homemade Teflon trough which was rotated at 8 rpm to reduce cumulative heating. The IR-pump/VSF-probe spectra were recorded under p/ssp (IR pump/VSF, VIS probe, IR probe) polarization. The IR pump pulse was variably delayed with

respect to the VSF probe signal using a mechanical delay line. The normalized VSF signal was computed as the ratio between the integrated intensities with and without the pump with an integrated bandwidth of 100 cm^{-1}.

Author contributions:

C.-S. H. and M. B. designed the research project. C.-S. H. performed the experiments. C.-S. H. and R. K. C. analyzed the data. Y. N. performed and analyzed the simulations. C.-S. H., R. K. C. and M. B. wrote the manuscript. All authors discussed the results and commented on the manuscript.

Acknowledgments:.

This work is part of the research program of the Stichting Fundamenteel Onderzoek der Materie with financial support from the Nederlandse Organisatie voor Wetenschappelijk Onderzoek.

1. Finlayson-Pitts BJ, James N. Pitts J (1999) *Chemistry of the Upper and Lower Atmosphere: Theory, Experiments, and Applications* (Academic Press).
2. Pijpers JJH, Winkler MT, Surendranath Y, Buonassisi T, Nocera DG (2011) Light-induced water oxidation at silicon electrodes functionalized with a cobalt oxygen-evolving catalyst. *Proc Natl Acad Sci USA* 108:10056–61.
3. Smits M et al. (2007) Ultrafast energy flow in model biological membranes. *New J Phys* 9:390–390.
4. Somorjai GA, Li Y (2010) *Introduction to Surface Chemistry and Catalysis* (John Wiley & Sons)second edi.
5. Wilson KR et al. (2002) Surface relaxation in liquid water and methanol studied by x-ray absorption spectroscopy. *J Chem Phys* 117:7738–7744.
6. Cappa CD, Smith JD, Wilson KR, Saykally RJ (2008) Revisiting the total ion yield x-ray absorption spectra of liquid water microjets. *J Phys: Condens Matter* 20:205105.
7. Aziz EF, Ottosson N, Faubel M, Hertel I V, Winter B (2008) Interaction between liquid water and hydroxide revealed by core-hole de-excitation. *Nature* 455:89–91.
8. Lewis T, Faubel M, Winter B, Hemminger JC (2011) CO2 capture in amine-based aqueous solution: role of the gas-solution interface. *Angew Chem Int Edit* 50:10178–81.
9. Bakker HJ, Skinner JL (2010) Vibrational spectroscopy as a probe of structure and dynamics in liquid water. *Chem Rev* 110:1498–517.
10. Piatkowski L, Eisenthal KB, Bakker HJ (2009) Ultrafast intermolecular energy transfer in heavy water. *Phys Chem Chem Phys* 11:9033–8.
11. Ramasesha K, Roberts ST, Nicodemus RA, Mandal A, Tokmakoff A (2011) Ultrafast 2D IR anisotropy of water reveals reorientation during hydrogen-bond switching. *J Chem Phys* 135:054509.
12. Asbury JB et al. (2004) Dynamics of water probed with vibrational echo correlation spectroscopy. *J Chem Phys* 121:12431–46.
13. Nibbering ETJ, Elsaesser T (2004) Ultrafast vibrational dynamics of hydrogen bonds in the condensed phase. *Chem Rev* 104:1887–1914.
14. Superfine R, Huang JY, Shen YR (1991) Nonlinear optical studies of the pure liquid/vapor interface: Vibrational spectra and polar ordering. *Phys Rev Lett* 66:1066–1069.
15. Shen Y (1989) Surface properties probed by second-harmonic and sum-frequency generation. *Nature* 337:519–525.
16. Byrnes SJ, Geissler PL, Shen YR (2011) Ambiguities in surface nonlinear spectroscopy calculations. *Chem Phys Lett* 516:115–124.
17. Ishiyama T, Morita A (2009) Vibrational Spectroscopic Response of Intermolecular Orientational Correlation at the Water Surface. *J Phys Chem C* 113:16299–16302.
18. Zhang W-K et al. (2005) Reconsideration of second-harmonic generation from isotropic liquid interface: broken Kleinman symmetry of neat air/water interface from dipolar contribution. *J Chem Phys* 123:224713.
19. Ni Y, Gruenbaum SM, Skinner JL (2013) Slow hydrogen-bond switching dynamics at the water surface revealed by theoretical two-dimensional sum-frequency spectroscopy. *Proc Natl Acad Sci USA* 110:1992–1998.
20. Raymond EA, Tarbuck TL, Brown MG, Richmond GL (2003) Hydrogen-bonding interactions at the vapor/water interface investigated by vibrational sum-frequency spectroscopy of HOD/H2O/D2O mixtures and molecular dynamics simulations. *J Phys Chem B* 107:546–556.
21. Sovago M et al. (2008) Vibrational response of hydrogen-bonded interfacial water is dominated by intramolecular coupling. *Phys Rev Lett* 100:173901.
22. Du Q, Superfine R, Freysz E, Shen YR (1993) Vibrational spectroscopy of water at the vapor/water interface. *Phys Rev Lett* 70:2313–2316.
23. Richmond GL (2002) Molecular bonding and interactions at aqueous surfaces as probed by vibrational sum frequency spectroscopy. *Chem Rev* 102:2693–724.
24. Gopalakrishnan S, Liu D, Allen HC, Kuo M, Shultz MJ (2006) Vibrational spectroscopic studies of aqueous interfaces: salts, acids, bases, and nanodrops. *Chem Rev* 106:1155–75.
25. Roberts ST, Ramasesha K, Tokmakoff A (2009) Structural rearrangements in water viewed through two-dimensional infrared spectroscopy. *Accounts Chem Res* 42:1239–1249.
26. Woutersen S, Bakker HJ (1999) Resonant intermolecular transfer of vibrational energy in liquid water. *Nature* 402:507–509.
27. Ashihara S, Huse N, Espagne A, Nibbering E, Elsaesser T (2006) Vibrational couplings and ultrafast relaxation of the O–H bending mode in liquid H2O. *Chem Phys Lett* 424:66–70.
28. Rey R, Møller KB, Hynes JT (2004) Ultrafast vibrational population dynamics of water and related systems: a theoretical perspective. *Chem Rev* 104:1915–28.
29. Pieniazek PA, Tainter CJ, Skinner JL (2011) Surface of liquid water: three-body interactions and vibrational sum-frequency spectroscopy. *J Am Chem Soc* 133:10360–3.
30. Gan W, Wu D, Zhang Z, Feng R, Wang H (2006) Polarization and experimental configuration analyses of sum frequency generation vibrational spectra, structure, and orientational motion of the air/water interface. *J Chem Phys* 124:114705.
31. McGuire JA, Shen YR (2006) Ultrafast vibrational dynamics at water interfaces. *Science* 313:1945–1948.
32. Smits M, Ghosh A, Sterrer M, Müller M, Bonn M (2007) Ultrafast Vibrational Energy Transfer between Surface and Bulk Water at the Air-Water Interface. *Phys Rev Lett* 98:098302.
33. Singh PC, Nihonyanagi S, Yamaguchi S, Tahara T (2012) Ultrafast vibrational dynamics of water at a charged interface revealed by two-dimensional heterodyne-detected vibrational sum frequency generation. *J Chem Phys* 137:094706.
34. Zhang Z, Piatkowski L, Bakker HJ, Bonn M (2011) Ultrafast vibrational energy transfer at the water/air interface revealed by two-dimensional surface vibrational spectroscopy. *Nat Chem* 3:888–93.
35. Hsieh C-S et al. (2011) Ultrafast Reorientation of Dangling OH Groups at the Air-Water Interface Using Femtosecond Vibrational Spectroscopy. *Phys Rev Lett* 107:116102.
36. Vila Verde A, Bolhuis PG, Campen RK (2012) Statics and dynamics of free and hydrogen-bonded OH groups at the air/water interface. *J Phys Chem B* 116:9467–81.
37. Chandler D (2005) Interfaces and the driving force of hydrophobic assembly. *Nature* 437:640–7.
38. Nagata Y et al. (2013) Water Bending Mode at the Water–Vapor Interface Probed by Sum-Frequency Generation Spectroscopy: A Combined Molecular Dynamics Simulation and Experimental Study. *J Phys Chem Lett* 4:1872–1877.
39. Nagata Y, Pool RE, Backus EHG, Bonn M (2012) Nuclear quantum effects affect bond orientation of water at the water-vapor interface (supporting information). *Phys Rev Lett* 109:226101.
40. Stiopkin IV et al. (2011) Hydrogen bonding at the water surface revealed by isotopic dilution spectroscopy. *Nature* 474:1–9.
41. Pieniazek PA, Tainter CJ, Skinner JL (2011) Interpretation of the water surface vibrational sum-frequency spectrum. *J Chem Phys* 135:044701.
42. Stenger J, Madsen D, Hamm P, Nibbering E, Elsaesser T (2001) Ultrafast Vibrational Dephasing of Liquid Water. *Phys Rev Lett* 87:027401.